研究論文

CO_2 아크 스폿 용접법에 의한 조립보의 굽힘강도에 관한 연구

한 명 수* · 한 종 만* · 이 준 열*

A Study on the Bending Strength of a Built-up Beam Fabricated by the CO_2 Arc Spot Welding Method

Myoung Soo Han* , Jong Man Han* and Jun Yul Lee*

Key Words : Car-carrying Ship (자동차 운반선), Arc Spot Welding (아크 스폿 용접), Built-up Beam (조립보), Stiffened Plate (보강 판), Effective Breadth (유효폭), Shear Fracture Strength (전단 파단강도), LIFTABLE Car Deck, LIGHT Car Deck

Abstract

In this study, bending test was performed on the real-scale, built-up beam test model fabricated by the CO_2 arc spot welding to evaluate the applicability of the welding method to the production of the stiffened plate in car-carrying ship. The built-up beam models which were fixed at both ends in longitudinal direction or simply supported to the rigid foundation, depending on the restraint condition of the corresponding car decks considered, were subjected to simulated design vehicle loads or concentrated point loads. During the test, the central deflection and the longitudinal bending stresses were measured from several points on the longitudinal flange face to predict the section properties of the built-up beams. The longitudinal bending stress on each spot weld were also measured to calculate the average horizontal shear force subjected to spot welds. Test results revealed that the shear strength of spot welds with their current weld nugget size and welding pitch was adequate enough to withstand the horizontal shear forces under the design vehicle loads. Although the built-up beam fabricated by the arc spot welding was a discontinuous beam, its mechanical behavior was well explained by

※ 1997년 4월 3일 접수, 1995년 춘계학술대회 발표

* Member, Daewoo Heavy Ind. Ltd.

the continuous beam theory using the effective breadth of plate. Based on test results, the criterion for the size of spot weld of which the average shear stress might meet the allowable stress requirement of AWS Code could be established.

1. INTRODUCTION

A stiffened plate is one of the principal structural elements in ship hull structures. In a car-carrying ship, cargo(car) decks are the typical structure of the stiffened plate, which has been conventionally fabricated by a continuous or intermittent fillet welding to join the longitudinal stiffener to the deck plate.

A few shipyards have applied the CO_2 arc spot welding, instead of an intermittent fillet welding, to improve productivity of the car deck where the design wheel weight is not very heavy.

This welding process is similar to the conventional CO_2 shielded gas metal arc welding (GMAW). Unlike GMAW, the CO_2 arc spot welding forms a stationary weld pool without moving a heat source. Because the welding heat is accumulated in a spot, a higher welding heat input can be expected by the CO_2 arc spot welding compared to the conventional GMAW[1].

In addition to joining the connected elements, the reinforcement of spot weld has an advantage of anti-skidding effect on the car at car deck without any special treatment.

From the design aspect of the stiffened plate with arc spot welds, two main issues related to strength of the structure are considered as follows :

1) Parameter for estimating the longitudinal strength and/or stiffness of the stiffened plate with arc spot welds.

2) Pitch and nugget size of welds for carrying the horizontal shear generated by lateral loads, especially design wheel load.

In the practical car deck design procedure, stress calculation to check design conformity on the longitudinal strength of a car deck has been generally done by considering only the section modulus of longitudinal stiffener. Although the deck plate is relatively thin, it actually affects the strength and stiffness of the deck structure. In simple beam theory, this portion is taken into account by introducing the effective breadth of the plate[2]. As might be expected, strength and stiffness of the stiffened plate with arc spot welds are influenced by pitch and nugget size of the welds. Thus, strength of the spot-welded structure will be different from that of the continuously welded structure. Therefore, it may be inadequate to applying the simple beam solutions obtained from continuous beams directly to the mechanical problems of the stiffened plate with arc spot welds.

To solve two issues submitted above, it is necessary to identify the stiffness of the plate represented such a form as the effective breadth. However, the stiffened plate with arc spot welds has not been fully reviewed in a viewpoint of strength and stiffness.

This study was performed by an experimental approach. Bend strength and stiffness for several built-up beam test models were reviewed to confirm the feasibility of applications of the CO_2 arc spot welding in real shipbuilding projects.

2 EXPERIMENTAL METHOD

2.1 Test materials

Table 1 shows the mechanical properties of materials used. Materials of the built-up beam for experiments are of AH36 grade steel according to the ABS classification with 6 mm thickness and A grade I-section beam with dimensions of 125 mm×

Table 1. Tensile properties of applied materials

Material	Steel grade	Y. S. (MPa)	T. S. (MPa)	Elongation (%)
Plate	AH36	410	511	26
I beam	A	353	462	24.8

60 mm×6 mm×8 mm. These materials were equally applied to the real car-carrying ships.

2.2 Test model and experimental method

Two types of car deck in a car-carrying ship were investigated for applying arc spot welding. One is a liftable car deck (LIFTABLE) and the other is the light car deck (LIGHT). Conventionally, they have been constructed using the intermittent fillet welds because of the small weight cars.

The built-up beams for experiments were prepared using the arc spot welding. The shape and dimensions of the test model are shown in Fig.

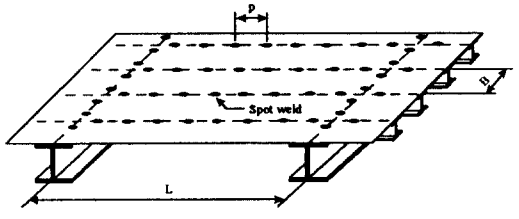

(a) Schematic of car deck structure

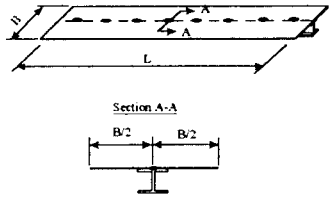

(b) Schematic of built-up beam test model

Fig. 1 Schematics of car deck and test model

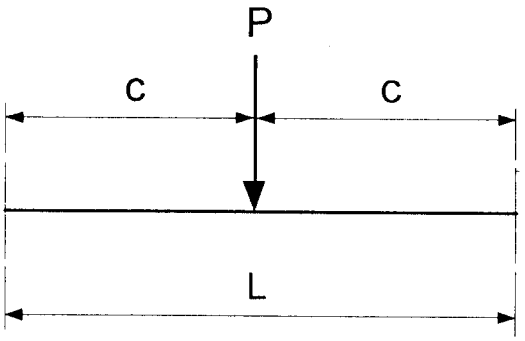

(a) Load type A in Table 2

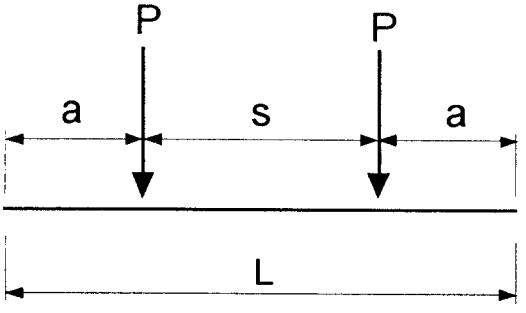

(b) Load type B in Table 2

Fig. 2 Schematics of loading condition

1. The span length L is a distance between the transverse deck girders and B is a distance between the longitudinal stiffener. The test model was designed to have the same dimensions and symmetries as the real car deck.

To assess load carrying capacity and safety in terms of strength of car decks under the design wheel load condition, the bending load tests were performed for the built-up beam with several loads and boundary conditions as shown in Table 2 and Fig. 2. These conditions are simulating the actual loads transferred to the car deck through the car wheels.

The load and boundary conditions assumed in structural design for car decks were of 30SS Two model for LIFTABLE and 48SC Two model for LIGHT, and design wheel load was 7.85 kN and 9.81 kN, respectively.

Table. 2 Test models according to test conditions for deck models

Deck	Test model ID	Length (mm)	Plate breadth (mm)	Boundary condition	Loading condition (1)			
					Load type	a (mm)	s (mm)	c (mm)
Liftable car deck	30SS-One	3000	780	Simple support	A	-		1500
	30SS-Two	3000	780	Simple support	B	782.5	1435	-
	30SC-One	3000	780	Fixed end	A	-	-	1500
	30SC-Two	3000	780	Fixed end	B	782.5	1435	-
Light car deck	48SS-Two	4800	810	Simple support	B	1600	1600	-
	48SC-Two	4800	810	Fixed end	B	1600	1600	-

(1) See Fig. 2

The welding procedures applied to the test model were shown in Table 3. Welding was performed through 2 steps. First step is related to the control of penetration and formation of nugget and second step is related to the crater treatment. The pitch between spot welds was uniformly maintained to be 400 mm. The number of spot welds was 8 in the LIFTABLE model and 11 in the LIGHT model.

Fig. 3 shows a configuration of test facility and test model set up. The steel frame and hydraulic actuator deliver loads to the test model which is constrained on the rigid foundation. The load level was evenly increased to the target value with increment of 2.5 kN.

The deflection and longitudinal bending stress at each load level were measured on the flange face of the longitudinal. Dial gauge (Scale division : 0.01 mm) and uniaxial strain gauge (Micro-measurement Group Inc., CEA-06-125UW-120) were used for measurements. Also, strain gauges were longitudinally attached on the center of each spot weld after grinding and polishing the reinforcement of welds.

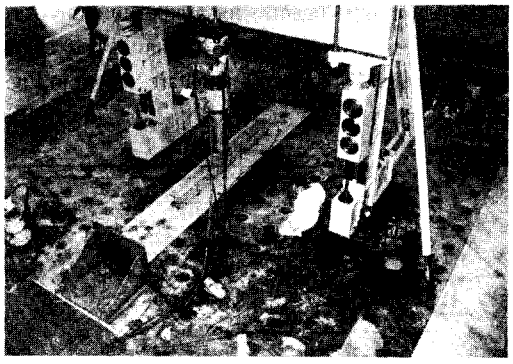

Fig. 3 Test facility and test model set up

Table. 3 CO_2 arc spot welding condition

Welding process	Polarity	Filler metal (1.2 mm)	Welding pitch (mm)	Welding parameters			
				Step	Amperes (A)	Voltage (V)	Time (Sec.)
GMAW (CO_2)	DCRP	ER70S-G (AWS)	400	1st	460	45	4.0
				2nd	230	29	1.5

3 RESULT & DISCUSSION

3.1 Spot weld

Fig. 4 shows a macro-structure of cross section of arc spot welds. The weld nugget was formed between deck plate and longitudinal member by the penetration of filler metal, and the reinforcement of spot welds would give an anti-skid effect to the deck plate.

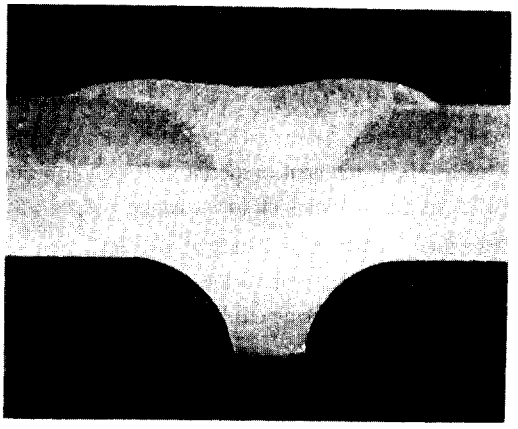

Fig. 4 Macrostructure of spot welds in transverse cross-section

Fig. 5 correlates the nugget diameter with the penetration depth of weld measured from test models after bend load test. The nugget diameter generally increases with increasing penetration depth. The average of nugget diameters measured was about 11.8 mm.

3.2 Bending characteristics of simply supported models

Fig. 6 shows the relationship between the central deflection (δ_M) and the applied load (P) for the test model being simply supported at both ends. In the case of 48SS-Two and 30SS-Two, the maximum load applied was 1.25 times of the

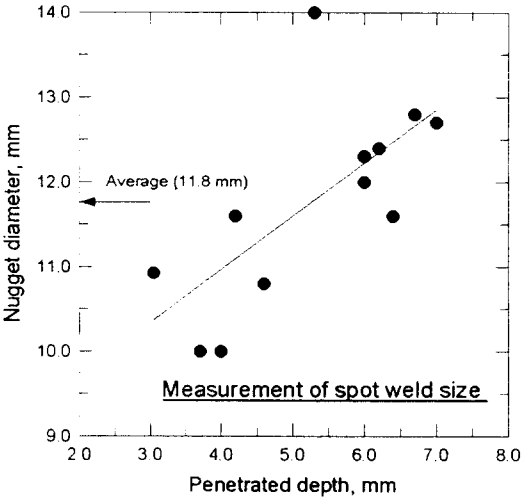

Fig. 5 Measurement of spot weld size for test models

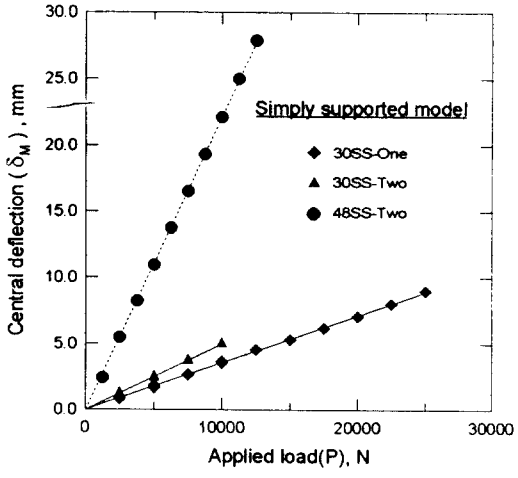

Fig. 6 Measurement of δ_M for simply supported models

design wheel load considering dynamic factor in service. In the case of 30SS-One, the maximum load applied was equal to the design vehicle load. The data show linear load-deflection relation, and thus, it can be expressed as Equation (1)

$$\delta_M = D_{M_S} P \quad (1)$$

where D_{Ms} is a experimental coefficient of proportionality in a simply supported beam. Coefficients, D_{Ms} were obtained from regression lines of data and shown in Table 4. Using the simple beam theory[3], D_{Ms} can be expressed as Equation (2)

$$D_{Ms} = a(3L^2 - 4a^2)/24EI_{cs}, \quad \text{for } 48SS-Two \text{ and } 30SS-Two$$
$$= L^3/48EI_{cs}, \quad \text{for } 30SS-One \tag{2}$$

where a and L are given in Table 2, and elastic constant, E, is assumed to 206 GPa, and I_{cs} is a moment of inertia in transverse cross section of a built-up beam.

Substituting the experimental coefficient D_{Ms}, a, and L into Equation (2) gives I_{cs} of each test model as shown in Table 4. Comparing I_{cs} values in Table 4 to the moment of inertia of I-section beam ($I_{Bs} \approx 3.94 \cdot 10^6$ mm^4), it is clearly noted that the increased values is due to the stiffness of plate joined to I-section beam. In the first place, it is assumed that the added stiffness can be represented by the effective breadth of plate in built-up beam.

Defining the dimension symbols of built-up beam as shown in Fig. 7, distance from the reference axis o-o to the neutral axis, y_c, is

$$y_c = (A_B \cdot g_B + A_P \cdot g_P)/A_T \tag{3}$$

where A_B is area of I-section beam, A_P is plate area, and A_T is A_B+A_P. Effective breadth of plate in terms of stiffness, b_{cs}, is

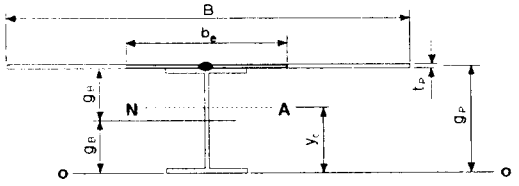

Fig. 7 Geometric symbols in built-up beam

$$b_{cs} = (\sqrt{B^2 - 4C} - B)/2 \tag{4}$$

In Equation (4), B and C are defined as Equation (5)

$$B = [A_B\{t_P^2 + 12(g_P - g_b)^2\} - 12(I_{cs} - I_{Bs})]/t_P^3$$
$$C = -12A_B(I_{cs} - I_{Bs})/t_P^4 \tag{5}$$

where I_{Bs} is moment of inertia of I-section beam. Also, section modulus on lower flange is $Z_{fs} = I_{cs}/y_c$. In this manner, the values of y_c, b_{cs}, and Z_{fs} for the simply supported models can be experimentally determined from P-δ_M relations as shown in Table 4.

The ratio b_{cs}/B of 48SS-Two was larger than that of 30SS-Two. This shows the dependence of effective breadth upon the span of built-up beam. 30SS-Two and 30SS-One of equal dimensions and different load condition resulted in different b_{cs}/B each other. It is a general trend, as reported, that the effective breadth of plate varies with dimensions of beam as well as load conditions[4,5].

The longitudinal bending stress (σ_M) on lower flange at the midsection of built-up beam is

$$\sigma_M = M_M/Z_{fs} = \lambda_s P \tag{6}$$

Table 4. Central deflection data and section properties of simply supported test models.

Test model ID	D_{Ms} ($\times 10^{-1}$)	I_{cs} (mm^4)	y_c (mm)	b_{cs} (mm)	Z_{fs} (mm3)	b_{cs}/B
30SS-One	3.56	$7.66 \cdot 10^6$	97.6	311.5	78438	0.40
30SS-Two	1.96	$7.83 \cdot 10^6$	99.3	344.4	78892	0.44
48SS-Two	22.15	$8.60 \cdot 10^6$	106.5	550.7	80750	0.68

where M_M is moment applied and λ_σ is a proportional coefficient. Substituting Z_{fc} into Equation (6) gives the estimated value of λ_σ. Also, λ_σ can be obtained by correlating σ_M measured at the midsection of test models with P. Table 5 shows comparison between the estimated and the experimental values of λ_σ. The experimental values of λ_σ are reasonably corresponding to the estimated values. This implies that the effective breadth in terms of stiffness is nearly same to that of strength.

Table 5. Comparison between experimental and estimated value of λ_σ

Test model ID	λ_σ ($\times 10^{-4}$)	
	Experiment	Estimation
30SS-One	9.38	9.56
30SS-Two	9.71	9.92
48SS-Two	19.07	19.82

For the stiffened plate, it has been reported that the effective breadth in terms of strength is larger than that of stiffness. Therefore, they need to be obtained together in order to characterize the stiffened plate in terms of both strength and stiffness[5]. Unlike general trends, this experiment revealed that the effective breadth of plate in simply supported beams was nearly equal in both case of strength and stiffness.

3.3 Bending characteristics of the fixed-end models

δ_M and σ_M of the fixed-end built-up beam (fixed-end beam) can be expressed as the form of Equations (1) and (6) as below

$$\sigma_M = \lambda_{\sigma \cdot P} = M'_M / Z_{fc} = (M_M - \alpha \cdot M_o)/Z_{fc} \quad (7)$$

$$\delta_M = D_{M\delta} \cdot P = D_{Ms} \cdot P - \alpha \cdot D'_M \cdot M_o \quad (8)$$

where M_o is end moment of the fully fixed-end beam, α is degree of constraint, M_S is central moment with the simply supported condition, D_M' is coefficient for moment term, and Z_{fc} is section modulus of the fixed-end beam.

In Equations (7) and (8), it can be observed that the proportional coefficients, $D_{M\delta}$ and λ_σ of the fixed-end beam are resultantly the functions of α and the effective breadth of plate (b_{ec}). The values of α and b_{ec} could be estimated using the relation between α and the effective breadth of plate[1,3] and the measured δ_M. Doing so, moment of inertia (I_{fc}), y_c, and section modulus (Z_{fc}) of fixed-end models are estimated as shown in Table 6.

A Comparison between Table 6 and Table 4 explains the dependence of the effective breadth upon the degree of constraint. That is, the effective breadth decreases with increasing degree of constraint.

Fig. 8 shows a graphical comparison of the measured and estimated results of δ_M and σ_M. And Table 7 shows a comparison of the measured and estimated coefficients of $D_{M\delta}$ and λ_σ in Equations (7) and (8). The estimated δ_M was nearly equal to the measured δ_M because of the effective breadth based on the measured value of δ_M. On the other hand, the estimated and measured σ_M showed

Table 6. Estimation for the fixed-end test models

Test model ID	α	b_{ec} (mm)	I_{fc} (mm^4)	y_c (mm)	Z_{fc} (mm^3)	b_{ec}/B
30SC-One	0.80	209	$6.92 \cdot 10^6$	91.1	75930	0.27
30SC-Two	0.80	253	$7.29 \cdot 10^6$	94.3	77350	0.32
48Sc-Two	0.89	385	$8.05 \cdot 10^6$	101.1	79700	0.48

Table 7. Test data and estimated results for the fixed-end test models

Test model ID	Experiment		Estimation	
	D_{Mc} ($\times 10^4$)	λ_c ($\times 10^3$)	D_{Mc} ($\times 10^4$)	λ_c ($\times 10^3$)
30SC-One	1.58	5.51	1.58	5.93
30SC-Two	1.95	3.45	1.93	4.25
48SC-Two	7.25	7.56	7.20	8.17

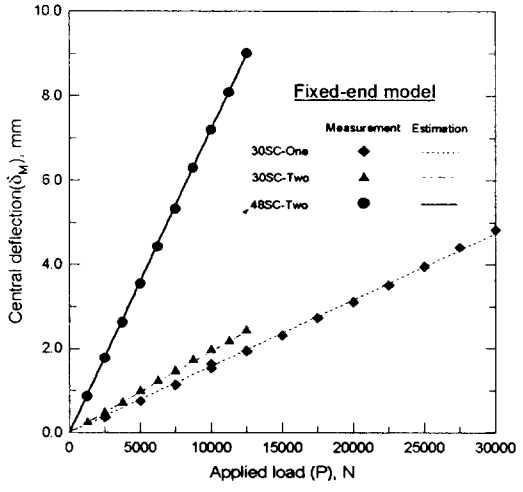

(a) Load - δ_M

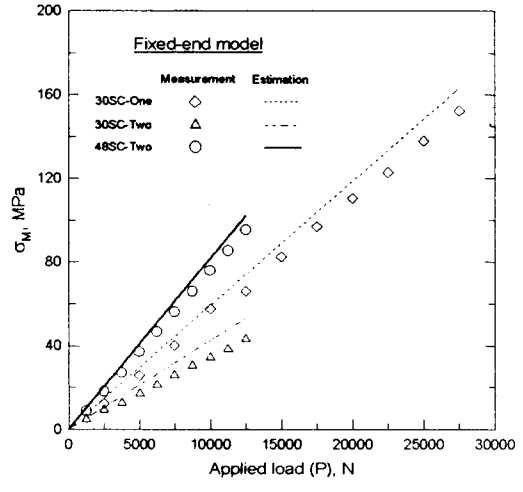

(b) Load - σ_M

Fig. 8 Comparison of the measured and the estimated of δ_M & σ_M for fixed-end model

some deviation, that is, the estimated was slightly higher than the measured. The maximum estimation error was about 23% in 30SC-Two model. These results imply that the effective breadth in terms of stiffness is different from that in terms of strength in the fixed-end beam, as reported previously[5]. But, this estimation method showed conservative results for σ_M.

3.4 Safety of the spot weld to shear fracture

To review the safety of the spot weld to shear fracture, a shear fracture test by tension was performed for the single spot welded lap joint specimens made of AH36 steel with 6 mm thickness.

Table 8 shows a summary of experimental results. The average shear fracture stress of arc spot welds was over the tensile strength of AH36 in Table 1.

Table 8. Shear fracture test result for spot welds

Specimen No.	Shear fracture strength, τ_f (Mpa)
1	573
2	542.8
Average	558

To estimate the shear stress on spot welds of test models, the shear flow, q which is the longitudinal shear force transmitted across the plane to the junction per unit length along the built-up beam is defined as Equation (9).

$$q = VQ / I_e \tag{9}$$

where V is the vertical shear force at a section, I_e is moment of inertia, and Q is the first moment of effective area equal to $b_e \times t_p$ in Fig. 7 about the neutral axis of the beam. The horizontal shear force at the contact plane between plate and I-

section beam within one pitch of spot weld (p) is simply given by Equation (10).

$$F = qp \tag{10}$$

Therefore, the horizontal shear stress at a spot weld having a nugget diameter, d is given by Equation (11).

$$\tau = 4F / \pi d^2 \tag{11}$$

Table 9 shows the estimation results obtained from Equations (9) through (11). 30SS-Two and 48SC-Two models are equivalent to the beam model in the structural design for LIFTABLE and LIGHT, respectively.

Table 9. Calculation of shear stresses in a spot weld by shear flow

Test model ID	V (kN)	Estimation results		
		F (kN)	τ (MPa)	τ_f / τ
30SS Two	7.85	23.78	217.5	2.6
48SC-Two	9.81	30.32	277.3	2.0

In Table 9, V is vertical shear force under the design load conditions for each car deck. In calculation, p is 400 mm, and d is 11.8 mm equal to the average value measured from test models (Fig. 5). The estimated shear stresses in a nugget at the design load conditions for each test model were under the half of τ_f in a single spot welded lap joint. From this, it is assessed that arc spot welds in two types of car deck can not be fractured by shear stress at the design load conditions and safety factor to shear fracture is higher than 2.0.

4 DISCUSSION

4.1 Considerations for the strength design of car deck with arc spot welds

Fig. 9 shows the distribution of longitudinal bending stress measured both on the lower flange face of I-section beam and on the center of the spot welds at the top surface of the plate for 30SS One model at the applied load 5, 10, 20, 25 kN.

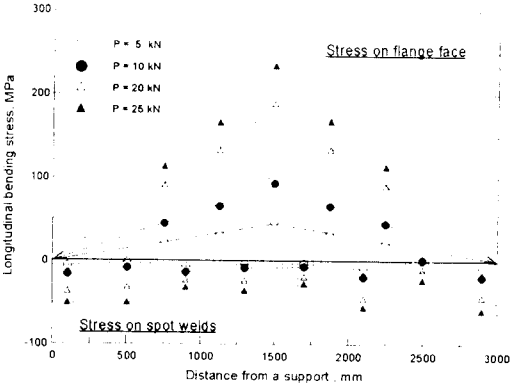

Fig. 9 Stress distribution along with beam span on spot weldsand flange face (30SS-One)

The stress measured on each spot weld comparatively remained constant regardless of the measuring location as shown in the beam subject to the pure bending without shear. This behavior indicates that the actual shear stress in the nugget of spot welds is much lower than the estimated value in Table 9.

On the other hand, the stress measured on the lower flange was in proportion to the moment arm at the measuring location. This explains that the stiffness of plate contributes uniformly to the total stiffness of built-up beam. From this, it is possible to conclude that the effective breadth of plate is available to the strength and stiffness calculation of the built-up beam with arc spot welds as well as the beam with continuous welds.

Furthermore, in test models equivalent to the beam model for the structural design of LIFTABLE (30SS-Two) and LIGHT (48SC-Two), σ_M at the design load was about 76.2 MPa and 74.2 MPa, respectively. These stresses were much lower than the allowable bending stress[6] for longitudinal

member of 175 MPa. Therefore, it is possible to conclude that the built-up beam with arc spot welds is sufficiently safe from the viewpoint of longitudinal strength.

4.2 Consideration for the arc spot weld size

From the viewpoint of the structural strength, spot welds are non-essential welds. It is acknowledged, however, that the extensive failure of these welds in service could lead to a very undesirable situation. Therefore, it is a reasonable concept that the requirement of the minimum weld size which guarantees the safety against the concerned failure mode needs to be established for spot welds.

To determine the minimum nugget diameter (d_w) of spot weld required for car deck structure, we considered the total area of welds which was effective for carrying the horizontal shear force in the single element of the stiffened plate. The allowable shear stress was determined in accordance with the AWS D1.1[7]. Supposing that the section properties of the built-up beam were not considerably changed by weld size, the value d_w could be defined as Equation (12).

$$d_w = 2 \cdot \sqrt{(QpV/\tau_w I_e - A_f/n)/\pi} \qquad (12)$$

where τ_w is the allowable shear stress, A_f is the effective throat area of double-sided fillet welds fabricated in both end connecting each longitudinal stiffener with transverse girder of car deck in lengths of 75 mm, equal to 850 mm^2, and n is number of spot welds.

According to AWS Code[7], the requirement of the allowable shear stress for the plug weld which is similar to arc spot weld is 0.3×nominal tensile strength of the filler metal. Based on this, the allowable shear stress of 168 MPa was determined.

Fig. 10 shows the relationship between d_w given by Equation (12) and wheel load for the case of LIFTABLE and LIGHT. The values, Q and I_e in Equation (12) were of 30SS-Two for LIFTABLE and 48SC-Two for LIGHT and p was 400 mm.

For the current design wheel load, 7.85 kN for LIFTABLE and 9.81 kN for LIGHT, Equation (12) gives d_w = 6.7 mm for LIFTABLE and d_w = 11.4 mm for LIGHT as shown in Fig. 10. By comparing these sizes with the nugget diameter measured from the test models as shown in Fig. 5, it was confirmed that the average of the nugget diameter measured, 11.8 mm, satisfies the minimum nugget size requirement for the design load conditions of car decks. Furthermore, the guidance for the minimum spot weld size corresponding to the design load in a similar structure could be determined by Equation (12) within the limited load range.

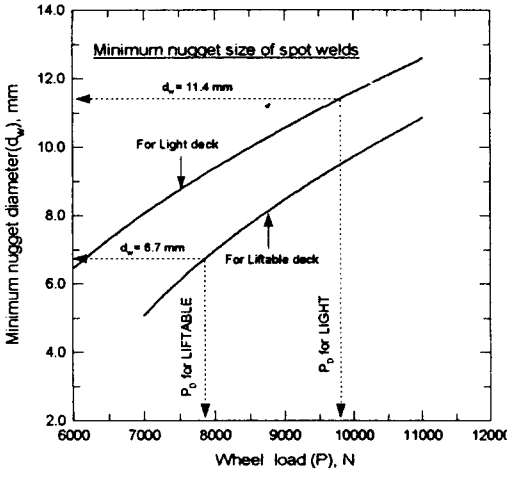

Fig. 10 Minimum nugget diameter of spot welds

5. CONCLUSION

In this study, the bend test for the built-up beams was performed to assess the load carrying capacity and safety in term of strength of the car decks fabricated by the CO_2 arc spot welding method. The results obtained are summarized as follows :

1) The concept of the effective breadth was available to the strength and stiffness calculations of the built-up beam with arc spot welds. In a simply supported built-up beam, the effective breadth of plate was even in terms of strength and stiffness. In a built-up beam of fixed ends, the effective breadth in terms of stiffness was slightly different from that of strength.

2) In test models which are designed equivalent to the beam model for the structural design of car decks (30SS-Two and 48SC-Two), the longitudinal bending stress at the midsection was much lower than the allowable bending stress for longitudinal member in ship because of the added stiffness of plate. Therefore, the built-up beam with arc spot weld was safe from the viewpoint of longitudinal strength.

3) The estimated shear stress in spot welds at the design load conditions of each car deck was under the half of shear fracture strength of a single spot welded lap joint. This means, in the arc spot welds in car decks, the safety factor to shear fracture is higher than 2.0.

4) By considering the total area of welds effective for carrying the horizontal shear force and the allowable shear stress in accordance with the AWS D1.1, the requirement of the minimum nugget diameter in the arc spot weld could be established. The average of nugget diameter measured from the test models satisfied the requirement.

REFERENCE

1. O. W. Blodgett : Calculating cooling rates of arc spot welds, Welding Journal, Vol. 66 (12), p. 17, (1987).
2. O. F. Hughes : Ship Structural Design, A Wiley-Interscience Pub., New York, pp. 121-124, (1983).
3. S. H. Crandall, N. C. Dahl, and T. J. Lardner : An Introduction to the Mechanics of Solids, McGraw-Hill Inc, (1978).
4. H. A. Schade : The effective breadth concept in ship structure design, Trans. SNAME, Vol. 61, pp. 410 - 424, (1953).
5. D. Boote, D. Mascia : On the effective breadth of stiffened plating, Ocean Engng. Vol. 18(6), pp. 567-592, (1991).
6. LR : Rules and Regulations, Part 3, Ship Structures, (1994).
7. AWS : ANSI/AWS D1.1-94, Structural Welding Code-Steel, p. 177, (1994).